Reactor scale-up in AOPs: from laboratory to commercial scale

C.S. Zalazar, M.D. Labas, C.A. Martín, R.J. Brandi and A.E. Cassano

INTEC (Universidad Nacional del Litoral and CONICET), Güemes 3450, (3000) Santa Fe, Argentina (E-mail: *acassano@ceride.gov.ar*)

Abstract A procedure to scale-up photoreactors employed in AOPs using laboratory information has been developed. Operating with a model compound the proposed procedure was applied to the decomposition of formic acid in water solution using hydrogen peroxide and UV radiation. With laboratory experiments the parameters of the kinetic equation were obtained in a small batch reactor operated within a recycling apparatus. The whole system was modeled employing radiation and mass balances. These balances were used together with a non-linear parameter estimator to derive the model kinetic constants. Then, these results were used in the modeling of the large-scale reactor to predict exit conversions in an isothermal, continuous, tubular flow reactor that is 2 m long and has a volume of 12 l. Once more, radiation and mass balances were used to predict formic acid output concentrations. Experimental data in the large-scale apparatus are in good agreement with theoretical predictions.

Keywords Formic acid; hydrogen peroxide; laboratory reactor; mathematical modeling; photochemical reactors; scale-up

Water Science and Technology **Vol 49 No 4 pp 13–18** © IWA Publishing 2004

Introduction

Photochemical reactors have a peculiar characteristic; it is almost impossible to build a reactor with a uniform concentration of photons in the reaction space. Spatial non-uniformities are intrinsic as a consequence of two different phenomena: (i) geometrical effects produced by cylindrical or spherical geometries and/or non-collimated illumination; and (ii) absorption of radiation by reactants and/or products and/or the catalyst. Although the first one can be avoided in laboratory reactors with special designs and Cartesian geometries, the second is unavoidable because without absorption by the reactant or the catalyst there is no reaction. This phenomenon leads to the existence of a whole field of spatially distributed reaction rates even in small apparatus. In other words, interpretation of laboratory reactor data needs a description of the radiation field much in the same way that this information is necessary for designing the large-scale system.

In this work we will show that with a detailed modeling of the laboratory reactor, it is possible to obtain a reaction kinetic model (and the corresponding kinetic parameters) that can be used to design, in the predictive mode, the performance of a large-scale reactor. The differences between these reactors are not only in their size but also in their operating conditions.

The aim of this work is to show the potential of mathematical modeling for scaling-up purposes; hence, in order to avoid complications with the chemistry of the system, we have chosen for this study a very simple model compound, formic acid. The decomposition of low concentrations of this substrate in water solution will be performed with a combination of hydrogen peroxide and low wavelength UV radiation.

Reaction kinetics

Equipment and operating conditions

In order to correctly characterize the kinetics, the reactor design must be as simple as

possible. From this point of view a flat plate configuration of cylindrical shape was chosen (see Figure 1). The complete circular cross-section of the reactor is fully irradiated from both sides. Two tubular, germicidal lamps having more than 90% of the output wavelengths in the 253.7 line produce irradiation. The cylindrical lamps are positioned at the focal lines of cylindrical reflectors of parabolic cross-section. In this way, with the choice of the appropriate geometric arrangement and dimensions, it will be possible to use a simple, one-dimensional radiation model (Alfano *et al.*, 1985). Both sides of the reactor are closed with circular quartz windows.

The reactor is placed inside a recycle which includes: (1) a high flow rate recirculating pump (to improve mixing and produce small conversion per pass in the reactor); (2) a heat exchanger for temperature control; and (3) a storage tank (for temperature measurement, mixing and sampling). The reactor volume is 70 ml and that of the tank is 2,000 ml.

The following variables were investigated: (1) the concentration of formic acid (from 40 to 140 ppm); (2) the molar ratio of hydrogen peroxide concentration to formic acid concentration (from 1.0 to 32); and (3) the average value of the LVRPA employing three different irradiation levels (by using two different lamps of 15 and 40 nominal power consumption and also interposing calibrated meshes between the irradiating system and the reactor). Distilled water was employed in all runs. The formic acid concentration in water was followed by means of ion chromatography measurements. Hydrogen peroxide was analyzed with colorimetric methods. The optical characteristic (absorbance) of the reacting mixture was controlled in all samples. Operating conditions were at steady state in all the parameters that were assumed constant: lamp operation, recirculating flow rate and temperature. The operating temperature was 20°C. Samples (30 cm^3) were taken from the tank at specific time intervals for the different analyses. With blank runs it was verified that there was no direct photolysis or direct attack of the formic acid by hydrogen peroxide without UV radiation.

In order to know the distribution of radiation inside the reactor a model was used as shown below. However, this model asks for the impinging incident radiation on each of the reactor windows (Martín *et al.*, 2000). These values were experimentally obtained by means of actinometric measurements employing the well-known potassium ferrioxalate actinometer.

Modeling the reaction kinetics

Experimental results have shown the following characteristics: (i) the kinetics of formic acid disappearance are independent of the formic acid concentration but depend on the hydrogen peroxide concentration; (ii) the oxygen concentration, within the limits of the investigated variables does not seem to affect the rate; (iii) the hydrogen peroxide degradation is a function of its concentration; (iv) the rate of disappearance of both compounds

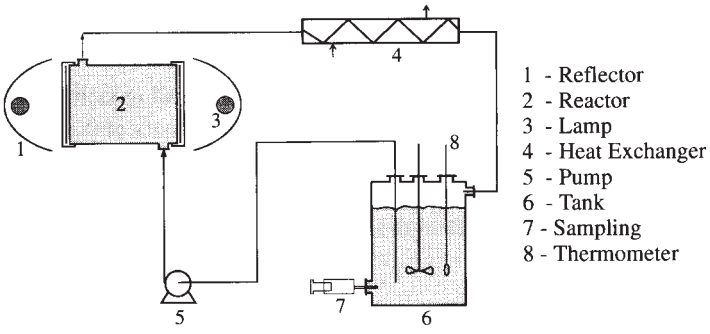

Figure 1 Schematic diagram for the laboratory reactor

depends linearly on the photon absorption rate. The following reaction sequence is proposed (Stefan and Bolton, 1998):

$$
\begin{array}{llllllll}
H_2O_2 + h\nu & \rightarrow & 2\,OH\bullet & & & & \phi & \\
H_2O_2 + OH\bullet & \rightarrow & HO_2\bullet + & H_2O & & & k_2 & \\
HO_2\bullet + OH\bullet & \rightarrow & H_2O + & O_2 & & & k_3 & \\
HO_2\bullet + HO_2\bullet & \rightarrow & H_2O_2 + & O_2 & & & k_4 & \\
HO_2\bullet + H_2O_2 & \rightarrow & H_2O + & O_2 + & OH\bullet & & k_5 & \\
OH\bullet + OH\bullet & \rightarrow & H_2O_2 & & & & k_6 & \\
OH\bullet + HCOOH + O_2 & \rightarrow\!\rightarrow & CO_2 + & H_2O + & HO_2\bullet & & k_7 = k'_7\, C_{O_2} & (1)
\end{array}
$$

Applying the local or micro steady-state approximation and considering that: (1) no square root dependence with the LVRPA has been observed; (2) $k_3 >> k_4$; (3) $k_5 << k_2$ and k_7; and (4) $k_2\, C_{HyPe}/k_6\, C_{For} \leq$ order 0.1, the following approximate kinetic model can be readily obtained:

$$R_{For}(x,t) = -k_1^*\, e_\lambda^a(x,t) \tag{2}$$

$$R_{HyPe}(x,t) = -k_2^*\, e_\lambda^a(x,t)\, r(t) \tag{3}$$

where k_1^* and k_2^* are lumped kinetic constants, e_λ^a (x, t) is the photonic absorption rate (a strong function of position) and $r = C_{HyPe}/C_{For}$. According to Eqs (2) and (3), only two parameters are needed to represent the kinetic model. These equations apply to local values of the reaction rates (because both are a function of x).

Laboratory reactor radiation and mass balances

In the way that the laboratory reactor is operated (good mixing and differential conversion per pass), it constitutes a special type of well mixed batch system with the peculiarity that there is reaction only in the irradiated part of it. The second aspect that must be taken into account is that measurements of concentrations in the samples taken from the tank, correspond to single values that represent the volume averaged result of the changes produced by spatially distributed reaction rates in the photochemical part of the reactor (because of the non-uniform radiation field). Thus, the mass balance must be written in terms of volume-averaged properties.

For the one-dimensional radiation field and a reactor illuminated from both sides, the radiation balance in terms of the photonic absorption rate gives the following expression for the local values:

$$e^a_{HyPe,\lambda}(x,t) = \kappa_{HyPe,\lambda} G_{w,\lambda} \left\{ \exp\left[-\left(\kappa_{HyPe,\lambda}(t)\right) x \right] + \exp\left[-\left(\kappa_{HyPe,\lambda}(t)\right)\left(L_R - x\right) \right] \right\} \tag{4}$$

Absorption by formic acid has been assumed negligible. κ is the absorption coefficient and G_w is the boundary condition that may be obtained with actinometric measurements as indicated before. This equation is written in terms of local values (a function of x). A single equation for λ = 254 nm is valid because we are using almost monochromatic radiation. Note that Eq. (4) is a function of time due to the variation of the absorption coefficient with the progress of the reaction (produced by the hydrogen peroxide consumption).

With the above considerations the mass balance results:

$$\frac{d\langle C_i \rangle_{V_R}(t)}{dt}\bigg|_{Tank} = \frac{V_R}{V_{Tot}} \left\langle R_{i,\lambda}(x,t) \right\rangle_{V_R} \tag{5}$$

In Eq. (5) i stands for either formic acid or hydrogen peroxide and $\langle\ \rangle$ denotes an average value. Note also that the reaction rate is preceded by the ratio of the photoreactor volume over the total volume. This coefficient results from the special type of batch reactor that is employed in this work. Eqs (2) or (3) must be substituted into Eq. (5). Each one of them calls for the value of $e^{a}_{HyPe,\lambda}(x, t)$ that is obtained from Eq. (4). Afterwards, the averaging integral must be performed for all properties that are a function of position. For a one-dimensional radiation model, the average extends over the x-coordinate (from 0 to L_R) and, in this case, we can obtain an analytical solution. The final result is a set of two ordinary differential equations that can be fed to a non-linear parameter estimator. The program compares for both, hydrogen peroxide and formic acid, the C vs. time experimental values with the predictions from the model and calculates the kinetic parameters. Within a 95% confidence interval the final results are:

$k^{*}_{For} = 0.3716 \pm 0.0114$ einstein/mol.
$k^{*}_{HyPe} = 0.0247 \pm 0.0087$ einstein/mol.

Scale-up

According to the method, the results shown above must be independent of the size, shape and operating conditions of the employed reactor. The validity of these constants can be verified by using them in the prediction of the performance of a reactor that is different in size, geometry and operation from the one used in the laboratory. With this purpose, a continuous flow, cylindrical reactor of annular cross-section, having a tubular lamp located at its centerline and operated at steady-state conditions will be used.

The reactor

The reactor was constructed in two separate sections each 1 m long (Figure 2); the reason being that commercial, readily available germicidal lamps have a length of 1.20 m. Each lamp has a nominal power consumption of 105 W. The annular cross-section for the reactor space resulted from two concentric tubes.

The first one was made of clear quartz having an outside diameter of 0.05 m. The second tube was made of Pyrex glass and has an inside diameter of 0.104 m. The lamp was placed coaxial with the tubes. The lamp, the inner and the outer tube were properly positioned by means of Teflon ends that had provisions for the incoming and outgoing streams. The reactor was fed by means of a centrifugal pump that was connected to a tank whose liquid level was kept constant. The whole system was operated at 20°C. Formic acid concentration was changed from 40 to 120 ppm and the ratio of hydrogen peroxide to formic acid was varied

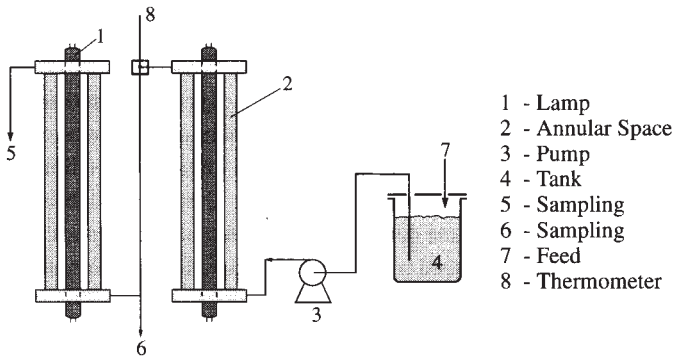

Figure 2 Schematic diagram for the commercial-scale reactor

from 2 to 10. The flowrate was measured at the exit sampling point by volumetric measurements. The system took about 30 minutes to reach steady operation. During this time the lamps were covered with an opaque tube. When steady state was achieved the masks were removed and the reaction started. Samples were taken at the intermediate and end outlets and were analyzed with the procedures described before.

Large-scale reactor radiation and mass balances

The general mass balance equation can be applied to the tubular reactor under the following assumptions and operating conditions: (i) steady state; (ii) unidirectional, incompressible, continuous flow of a Newtonian fluid; (iii) only ordinary diffusion is significant; (iv) azimuthal symmetry; (v) axial diffusion neglected as compared to the convective flow; and (vi) constant physical and transport properties. The following model equation in cylindrical coordinates (r, z) holds:

$$v_z(r)\frac{\partial C_i(z,r)}{\partial z} - \mathrm{D}_{im}\left[\frac{1}{r}\frac{\partial}{\partial r}\left(r\frac{\partial C_i(z,r)}{\partial r}\right)\right] = R_{\mathrm{Hom},i}(z,r) \tag{6}$$

where v_z is the velocity distribution in the annular space and D_{im} is the diffusivity of the i species in the mixture. This equation must be integrated with the following initial and boundary conditions:

$z = \ 0$ and every $r \quad C_i = C_{i,0}$
$r = r_{R,\mathrm{i}}$ and every $z \quad \delta C_i/\delta r = 0$
$r = r_{R,\mathrm{o}}$ and every $z \quad \delta C_i/\delta r = 0$

$r_{R,\mathrm{i}}$ and $r_{R,\mathrm{o}}$ are, respectively, the inner and outer radius of the annular reactor. The velocity v_z can be obtained with a momentum balance with the same assumptions that were described for the mass balance. However, one must keep in mind that the obtained equation (with the classical distorted parabolic profiles in the annular space) will hardly be a good assumption because of the impossibility of obtaining a fully developed velocity profile in both reactors. In spite of it, the analytical solution will be used knowing that it will be the weakest part of the analysis.

In the right-hand side of Eq. (6) we must insert the results of the kinetic models with the kinetic parameters obtained in the laboratory reactor. The resulting equation, with the initial and boundary conditions must be solved numerically. The solution of the two partial differential equations provides formic acid and hydrogen peroxide exit concentrations as a function of the radial position. In order to compare these results with data from the actual reactor and considering the velocity distribution of the outgoing flow, the mixed-cup or flowrate-averaged concentration must be calculated.

Once more, we need a model for the photon distribution in the annular space. It can be obtained with an emission model for the lamp (Cassano *et al.*, 1995), the optical characteristics of the reactor wall, the optical characteristics of the reaction space and the geometrical dimensions of the lamp–reactor system. The emission produced by a small volume element of the lamp along the direction θ, ϕ that arrives at the reactor at $s = s_R$ and reaches a point of incidence Inc.$(\boldsymbol{x})$ inside the reactor, in terms of the specific intensity, is:

$$I_\lambda(\boldsymbol{x},\theta,\phi,t) = I_\lambda^0(\theta,\phi,t)\ \ \exp\left[-\int_{\bar{s}=s_R(\boldsymbol{x},\theta,\phi)}^{\bar{s}=s_I(\boldsymbol{x},\theta,\phi)} \kappa_{\mathrm{HyPe},\lambda}(\bar{s},t)\mathrm{d}\bar{s}\right] \tag{7}$$

where $I_\lambda^0(\theta, \phi, t)$ is the boundary condition for I_λ at the point of entrance and for an arbitrary direction Ω. θ and ϕ are spherical coordinates of a system having their origin at the point of incidence, Inc. This boundary condition is provided by the lamp emission model, has been

developed by Cassano *et al.* (1995) and has the following value for steady irradiation:

$$I_{\lambda}^{0}(\theta,\phi) = \frac{P_{S,\lambda}}{4\pi^2 R_L^2 L_L} \frac{\left(R_L^2 - r^2 \sin^2\phi\right)^{1/2}}{\sin\theta} Y_{R,\lambda}(\theta,\phi) \tag{8}$$

In Eq. (8) $P_{S,\lambda}$ is the lamp output power at wavelength λ (photons per second), R_L is the lamp radius, L_L is the useful lamp length and $Y_{R,\lambda}$ is a compounded transmission coefficient of the reactor wall (considering absorption and reflections). The next step is to integrate all possible contributions (directions) of irradiation from the lamp volume of emission to the point Inc. ($\boldsymbol{x}$). Transforming the specific intensities into the photon absorption rate, the following result is obtained:

$$e_{\lambda}^{a}(\boldsymbol{x},t) = \kappa_{\mathrm{HyPe},\lambda}(\boldsymbol{x},t) \int_{\phi_1}^{\phi_2} d\phi \int_{\theta_1(\phi)}^{\theta_2(\phi)} d\theta \sin\theta \, I_{\lambda}^{0}(\theta,\phi,t) \quad \exp\left[-\int_{\bar{s}=s_R(x_0,\theta,\phi)}^{\bar{s}=s_{\mathrm{Inc.}}(\boldsymbol{x},\theta,\phi)} \kappa_{\mathrm{HyPe},\lambda}(\bar{s},t) d\bar{s} \right] \tag{9}$$

In the double integral θ accounts for the lamp length and ϕ for the lamp diameter. The integration limits were derived by Cassano *et al.* (1995).

Equation (9) must be inserted into the kinetic models. The numerical solution of the resulting equation gives formic acid and hydrogen peroxide concentrations as a function of position. At $z = L_R$ (the reactor length) the flowrate averaging procedure eliminated the dependence on r, and the predicted results can be compared with experimental values. The following results in terms of exit conversions were obtained:

Run	C_F (ppm)	r	$x_{\mathrm{Pred.}}$	$x_{\mathrm{Exp.}}$	% error
1	46	2	19.0	17	11.8
2	92	2	19.2	23.5	18.3
3	110	7.5	32.7	35	6.6

These results are quite satisfactory.

References

Alfano, O.M., Romero, R.L. and Cassano, A.E. (1985). A cylindrical photoreactor irradiated from the bottom I. Radiation flux density generated by a tubular source and a parabolic reflector. *Chem Eng. Sci.*, **40**(11), 2119–2127.

Cassano, A.E., Martín, C.A., Brandi, R.J. and Alfano, O.M. (1995). Photoreactor analysis and design: fundamentals and applications – a review. *Ind. Eng. Chem. Res.*, **34**, 2155–2201.

Martín, C.A., Alfano, O.M. and Cassano, A.E. (2000). Decolorization of water for domestic supply employing UV radiation and hydrogen peroxide. *Catal. Today*, **60**(1–2), 119–127.

Stefan, M.I. and Bolton, J.R. (1998). Mechanism of the degradation of 1,4-dioxane in dilute aqueous solution using the UV/hydrogen peroxide process. *Environ. Sci. Technol.*, **32**(11), 1588–1595.